Fractional
Differential
Calculus
Volume 15, Number 1 (2025), 53–69 doi:10.7153/fdc-2025-15-04

CHAOTIC DYNAMICS AND CHAOS CONTROL IN A FRACTIONAL–ORDER 2D CHAOTIC MAP BASED ON THE CAPUTO DIFFERENCE OPERATOR

HANECHE NABIL* AND HAMAIZIA TAYEB

(*Communicated by F. Atici*)

Abstract. In the last few years, there has been significant interest in the literature of fractional calculus and its applications in nonlinear dynamical systems. This is especially true in fields such as physics, chemistry, biology, and engineering. This paper presents a fractional-order two-dimensional rational chaotic map. Using the Caputo-like delta difference operator, the fractional-order counterpart is constructed. By varying the system parameters and fractional order, the proposed fractional map can exhibit complex dynamic behavior. The chaotic dynamics are investigated by adopting several classical tools such as phase plots, bifurcation diagrams, the maximum Lyapunov exponent spectrum, and dynamical maps. In addition, the 0-1 test algorithm is presented to validate the chaotic behavior of the fractional map. In order to evaluate the complexity level of the fractional map, the C_0 algorithm and spectral entropy are employed. Finally, a nonlinear control law is designed to stabilize the state trajectories of the chaotic map towards zero. Computer simulations are carried out to illustrate and validate the theoretical results obtained in this paper.

1. Introduction

Fractional calculus plays a critical role in several fields of science. The practical application of fractional-order systems is now known as an important field in engineering [21]. Leibniz introduced the first concept of a fractional-order equation in a letter he wrote in 1695, and research on it is still ongoing. This field of research has long remained theoretical, without practical application. Deficit computing has captured the attention of many researchers in recent decades. New studies show that fractional-order equations may explain many phenomena with more accuracy than integer-order equations, providing an efficient tool for describing the structures of systems displaying complex dynamics. Although we view their approximations as integers, many natural systems adhere to fractional dynamics [19]. Several academic fields have applied fractional-order systems in the last few years. For instance, fractional-order systems find application in physics fields such as nonlinear optics and quantum mechanics [25], in electronics fields such as electromagnetic waves, electrodynamics, and electrical circuits [23], and in medical and biological sciences fields such as HIV infection modeling,

Mathematics subject classification (2020): 26A33, 37D45, 68Q87, 34H10.
Keywords and phrases: Chaotic map, Caputo-like operator, spectral entropy, chaos control.
* Corresponding author.

Paper FDC-15-04

muscle blood vessel modeling, and the movement and foraging behavior of microorganisms [11]. Furthermore, the literature has extensively explored the important role of fractional-order equations in control engineering and renewable energy [17].

Chaotic behavior has been discovered in different scientific fields, including biology, epidemiology, mechanics, physics, neural networks, lasers, medicine, finance, and secure communication [10]. A chaotic system, a nonlinear system, exhibits a sensitive dependence on initial conditions. A small change in the initial conditions can lead to completely different outcomes. The Lyapunov exponent can measure the convergence or divergence of nearby trajectories in a deterministic dynamical system. The existence of a positive Lyapunov exponent indicates that the system exhibits chaotic behavior [8]. Discrete maps gained considerable interest in the investigation of dynamical systems. Discrete maps manifest in several fields, including cryptography, signal processing, neurology, diffusion, and infectious diseases [12]. Recent findings showed that simple first-order nonlinear maps may produce complex dynamical behavior, including chaos. Fractional chaotic maps, exhibiting more complex dynamics than their integer-order counterparts, can enhance security, making them more appropriate for use in various fields such as electronics, communications, and cryptography. Further, discrete fractional operators introduce a memory effect, which can capture the history of the states of the system. The fractional chaotic maps often display rich dynamical behaviors, such as the coexistence of attractors, which can be useful for various applications in control systems and signal processing. In addition, the fractional chaotic maps offer flexibility in control and synchronization. These properties motivate the detailed study of a fractional chaotic map in this paper. Recently, several fractional chaotic maps have been constructed using discrete fractional operators, such as the fractional logistic map [26], fractional Hénon map [15], fractional Lozi map [16], and fractional Tinkerbell map [4]. The stability of fixed points is crucial while examining chaotic maps. The researchers aimed to determine fixed points and examined the dynamics of orbits near these fixed points. Recent research has shown that classical chaotic maps often exhibit unstable fixed points. Due to their efficiency, accuracy, and speed for simulation, using discrete-time dynamical systems for modeling real-world phenomena is more suitable than continuous-time systems [18]. The fractional maps are therefore more suitable for image encryption and secure communication since they incorporate a higher level of flexibility. Further, using fractional maps for modeling biological phenomena allows capturing memory effects and hereditary properties [13]. Typically, fractional-order maps exhibit simpler structures while displaying more complex dynamical features than their integer-order counterpart.

Researchers have recently investigated several dynamics, including chaos, hyperchaos, and coexisting attractors in fractional-order maps. The hyperchaotic dynamics of the fractional generalized Hénon map have been examined [22]. A new variable-order fractional chaotic system has been presented in [28], where the logistic, Hénon, and Chen fractional systems have been studied. In addition, the proposed models have been applied to block image encryption with different fractional orders. Wu et al. [29] have investigated the data-driven learning of fractional difference equations, where a multi-layer neural network has been designed. Further, the proposed method has been applied to parameter estimation of one- and two-dimensional fractional chaotic systems. In [9], the authors described the chaotic behavior of a new fractional-order map with an infinite line of equilibria. In [7], Feng et al. constructed a new fractional-order 3D Lorenz chaotic system and a robust 2D sinusoidally constrained polynomial hyperchaotic map. Further, they developed an efficient multi-image encryption algorithm based on the new fractional-order maps to ensure a high level of security. Several fields of study have intensively studied fractional-order iterated maps due to their specific dynamic properties. Based on these considerations and motivated by the above discussions, we consider in the current paper a 2D fractional map and we focus on the study of the effect of system parameters and the fractional order on the dynamic behaviors of this discrete system. The existence of chaotic attractors is confirmed using bifurcation diagrams, the maximum Lyapunov exponent, and the 0-1 test method. Furthermore, we rigorously analyze and explore the complexity, which represents the irregularity in the discrete data, and the entropy, which measures the degree of regularity and unpredictability of data fluctuations.

The key contributions of the study are summarized as follows:

- Constructing a fractional-order map based on the Caputo-like delta operator and designing a convenable numerical scheme for computer simulations.

- Investigating the dynamical behavior of the proposed map and exploring the effect of the system parameters and the fractional order on the global dynamics of this discrete system.

- Designing a very simple nonlinear control law for stabilizing the state trajectories of the chaotic fractional map.

- Rigorous approach using the stability theory of discrete-time fractional systems.

The remainder of this paper is organized as follows: In Section 2, basic notions of discrete fractional calculus are introduced. Section 3 presents the proposed 2D fractional map, which is constructed using the Caputo discrete operator. In Section 4, the dynamical behavior of the fractional map is investigated. In Section 5, the 0-1 test technique is presented to confirm the existence of chaos in the proposed fractional map. In addition, the complexity of the fractional map is evaluated by adopting the C_0 algorithm and spectral entropy measure. Section 6 deals with the chaos control of the fractional map, where a simple nonlinear controller is designed to stabilize the state trajectories of the chaotic discrete system. We draw conclusions in Section 7.

2. Mathematical background

In this section, we will recall some basic notions of discrete fractional calculus that help us build this manuscript. We shall use the time scale $\mathbb{N}_\theta = \mathbb{N}_0 + \{\theta\} = \{\theta, \theta+1, \theta+2, \ldots\}$ where $\theta \in \mathbb{R}$.

DEFINITION 1. [3] Let $\xi : \mathbb{N}_\theta \to \mathbb{R}$ be a real-valued function. For $\nu > 0$, the ν^{th}-order fractional sum of ξ is defined as

$$\Delta_\theta^{-\nu}\xi(t) = \frac{1}{\Gamma(\nu)} \sum_{s=\theta}^{t-\nu} (t-s-1)^{(\nu-1)}\xi(s), \tag{1}$$

where $t \in \mathbb{N}_{\theta+\nu}$. The term $t^{(\nu)}$ is the falling factorial function given by

$$t^{(\nu)} = \frac{\Gamma(t+1)}{\Gamma(t+1-\nu)} = t(t-1)\dots(t-\nu+1). \tag{2}$$

DEFINITION 2. [1] The Caputo-like fractional difference operator of a function ξ is defined as

$${}^C\Delta_\theta^\nu \xi(t) = \Delta_\theta^{-(m-\nu)}\Delta^m \xi(t) = \frac{1}{\Gamma(m-\nu)} \sum_{s=\theta}^{t-(m-\nu)} (t-s-1)^{(m-\nu-1)}\Delta_s^m \xi(s), \tag{3}$$

where $\nu \notin \mathbb{N}$, $m = [\nu]+1$, and $t \in \mathbb{N}_{\theta+m-\nu}$.

For the integer case, the Caputo delta difference fractional operator simplifies to the traditional difference operator. Thus, when the fractional order ν is an integer, the Caputo delta difference fractional operator reduces to the standard forward difference operator, which is defined as

$$\Delta\xi(t) = \xi(t+1) - \xi(t), \tag{4}$$

and for an integer order n, the Caputo delta difference is given by

$$\Delta^n \xi(t) = \Delta\left(\Delta^{n-1}\xi(t)\right). \tag{5}$$

This means that the operator is applied repeatedly n times, which corresponds to the $n-$th order difference.

In order to obtain the numerical scheme of a fractional-order map, we will use the following theorem.

THEOREM 1. [6] *Given the Caputo's like discrete initial value problem*

$$\begin{cases} {}^C\Delta_\theta^\nu \xi(t) = g(t+\nu-1, \xi(t+\nu-1)), & t \in \mathbb{N}_{\theta+m-\nu}, \\ \Delta^k \xi(\theta) = \xi_k, \quad m = [\nu]+1, & k = 0,1,2,\dots,m-1, \end{cases} \tag{6}$$

then the unique solution of problem (6) *is given by*

$$\xi(t) = \xi_0(t) + \frac{1}{\Gamma(\nu)} \sum_{s=\theta+m-\nu}^{t-\nu} (t-s-1)^{(\nu-1)} g(s+\nu-1, \xi(s+\nu-1)), \quad t \in \mathbb{N}_{\theta+m}, \tag{7}$$

where

$$\xi_0(t) = \sum_{k=0}^{m-1} \frac{(t-\theta)^{(k)}}{\Gamma(k+1)} \Delta^k \xi(\theta). \tag{8}$$

In order to establish the stability conditions of the equilibrium points of a discrete-time fractional-order system, we will recall the following theorem.

THEOREM 2. [5] *The zero equilibrium point of the discrete-time fractional-order system*

$$^{C}\Delta_{\theta}^{\nu}S(t) = MS(t+\nu-1), \quad \nu \in (0,1], \tag{9}$$

where $S(t) = (s_1(t), s_2(t), \ldots, s_n(t))^T$, $M \in \mathbb{R}^{n\times n}$ *and* $t \in \mathbb{N}_{\theta+1-\nu}$ *is asymptotically stable if*

$$\lambda_j \in \left\{ \eta \in \mathbb{C} : |\eta| < \left(2\cos\frac{|\arg\eta| - \pi}{2-\nu}\right)^{\nu} \quad \text{and} \quad |\arg\eta| > \nu\frac{\pi}{2} \right\}, \quad j = 1,2,\ldots,n \tag{10}$$

where λ_j *are the eigenvalues of the matrix* M.

3. Mathematical model

In [2], S. Askar et al. proposed the following 2D rational chaotic map

$$\begin{cases} x(m+1) = x(n) + k(x(m))^2\left(\alpha - \gamma - \beta\frac{x(m)}{x(m)+y(m)} - \beta\log\left(x(m)+y(m)\right)\right), \\ y(m+1) = y(n) + k(y(m))^2\left(\alpha - \gamma - \beta\frac{y(m)}{x(m)+y(m)} - \beta\log\left(x(m)+y(m)\right)\right), \end{cases} \tag{11}$$

where x and y are the state variables. α, β, γ, and k are positive constants. For $\alpha = 2$, $\beta = 0.5$, $\gamma = 0.5$, $k = 0.87$, and the initial conditions $(x_0, y_0) = (0.21, 0.22)$, the integer-order 2D rational map (11) behaves chaotically as shown in Fig. 1, where the time series of $x(n)$ is depicted in Fig. 1(a) and the chaotic attractor is depicted in Fig. 1(b).

m

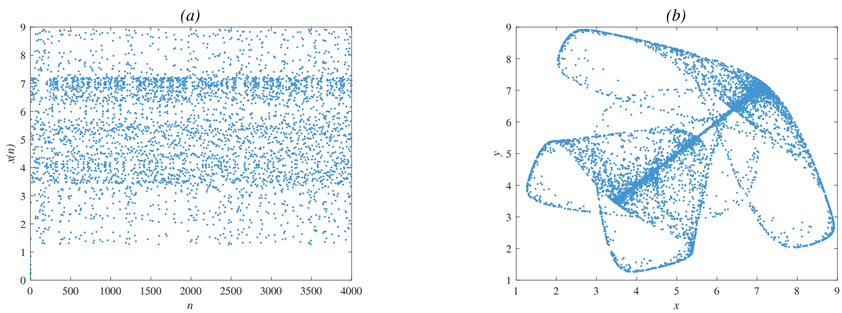

Figure 1: *Chaotic behavior of the integer-order map (11): (a) Time series of* $x(n)$*; (b) Phase portrait in* (x,y)*-plane.*

In order to examine the impact of the parameter k on the dynamics of integer-order map (11), we vary k in the range $[0.6, 0.9]$. The results of bifurcation diagram and maximum Lyapunov exponent (MLE) when k varies are represented in Fig. 2(a) and 2(b), respectively. From the bifurcation diagram, the map (11) exhibits chaotic behavior in the range $k \in [0.85, 0.9]$. This finding is validated by the maximum Lyapunov exponent spectrum. As one can see, the MLE is positive when k ranges between $0.85 \leqslant k \leqslant 0.9$ and then the discrete system (11) has rich dynamic behavior when the parameter k is varied.

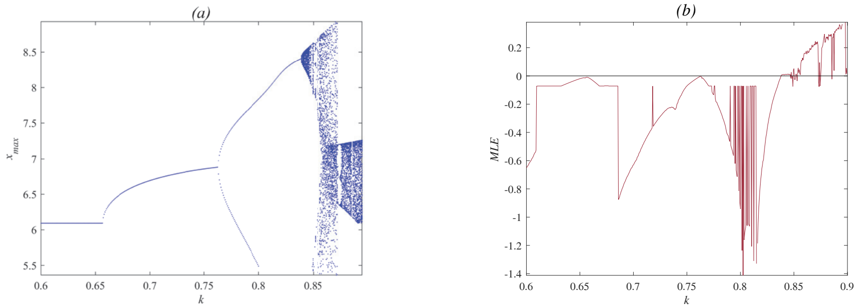

m

Figure 2: *Dynamics of the integer-order map* (11)*: (a) Bifurcation diagram with respect to* k*; (b) Maximum Lyapunov exponent spectrum with respect to* k*.*

In order to investigate the dynamic behavior of the discrete system (11) more accurately, the first-order difference of the discrete system (11) is given by

$$\begin{cases} \Delta x(m) = k(x(m))^2 \left(\alpha - \gamma - \beta \frac{x(m)}{x(m)+y(m)} - \beta \log(x(m)+y(m))\right), \\ \Delta y(m) = k(y(m))^2 \left(\alpha - \gamma - \beta \frac{y(m)}{x(m)+y(m)} - \beta \log(x(m)+y(m))\right). \end{cases} \tag{12}$$

Based on the Caputo-like delta operator, the fractional counterpart of the discrete system (11) with order $\nu \in (0,1]$ can be obtained as

$$\begin{cases} {}^{C}\Delta_{\theta}^{\nu} x(t) = k(x(t-1+\nu))^2(\alpha - \gamma - \beta \dfrac{x(t-1+\nu)}{x(t-1+\nu)+y(t-1+\nu)} \\ \qquad\qquad - \beta \log(x(t-1+\nu)+y(t-1+\nu))), \\ {}^{C}\Delta_{\theta}^{\nu} y(t) = k(y(t-1+\nu))^2(\alpha - \gamma - \beta \dfrac{y(t-1+\nu)}{x(t-1+\nu)+y(t-1+\nu)} \\ \qquad\qquad - \beta \log(x(t-1+\nu)+y(t-1+\nu))), \end{cases} \tag{13}$$

where θ is the starting point and $t \in \mathbb{N}_{\theta+1-\nu}$. Using theorem (1) and assuming that $\theta = 0$, the numerical scheme of the fractional system (13) is obtained as

$$\begin{cases} x(m) = x(0) + \dfrac{1}{\Gamma(\nu)} \displaystyle\sum_{j=1}^{m} \dfrac{\Gamma(m-j+\nu)}{\Gamma(m-j+1)} (k(x(j-1))^2(\alpha - \gamma - \beta \dfrac{x(j-1)}{x(j-1)+y(j-1)} \\ \qquad - \beta \log(x(j-1)+y(j-1)))), \\ y(m) = y(0) + \dfrac{1}{\Gamma(\nu)} \displaystyle\sum_{j=1}^{m} \dfrac{\Gamma(m-j+\nu)}{\Gamma(m-j+1)} (k(y(j-1))^2(\alpha - \gamma - \beta \dfrac{y(j-1)}{x(j-1)+y(j-1)} \\ \qquad - \beta \log(x(j-1)+y(j-1)))), \end{cases} \tag{14}$$

where $x(0)$ and $y(0)$ are the initial conditions. This numerical scheme allows us to examine the sensitivity of the fractional map (13) in the remainder of this paper.

4. Dynamics of the fractional-order map

In this section, the dynamics of the fractional-order map (13) are investigated using several classical tools, such as bifurcation diagrams, maximum Lyapunov exponent spectrum, phase plots, and dynamical maps.

In bifurcation diagram, we vary one of the system parameters and fixing the others parameters in to explore the chaotic dynamics of the system. Generally, a chaotic system is sensitive to variation of its parameters and initial conditions. Let the parameter k vary from 0.5 to 0.9 and fix $\alpha = 2$, $\beta = 0.5$, $\gamma = 0.5$, and the fractional order $\nu = 0.62$. The bifurcation diagram of the fractional-order map (13) and the correspoding maximum Lyapunov exponent spectrum with respect to k are depicted in Figs. 3(a) and 3(b), respectively. It sould be noted that the maximum Lyapunov exponent for a fractional map can be estimated using the Jacobian matrix algorithm; see [27].

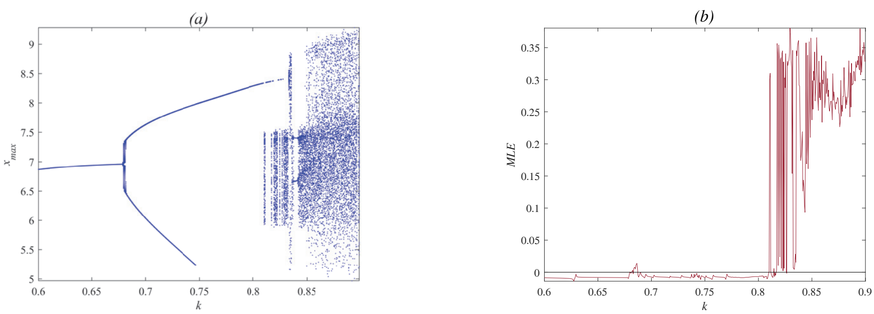

Figure 3: *Dynamics of the fractional-order map* (13) *as* k *varies: (a) Bifurcation diagram with respect to* k*; (b) Maximum Lyapunov exponent spectrum with respect to* k.

As one can see, the fractional map (13) is periodic when $k \in [0.6, 0.85]$ which indicated by the negative values of the maximum Lyapunov exponent, but when k increases, the dynamics of the fractional map (13) becomes very complex or chaotic. Thus, the impact of the parameter k on the dynamics of the fractional map (13) is investigated.

Now, we study the effect of the fractional order ν on the dynamic behavior of the fractional map (13). Fix $\alpha = 2$, $\beta = 0.5$, $\gamma = 0.5$, and $k = 0.87$ and let ν vary from 0 to 1. Fig. 4 shows the bifurcation diagram and the corresponding maximum Lyapunov exponent spectrum. By examining the bifurcation diagram and the MLE spectrum depicted in Fig. 4, it is shown that the fractional map (13) takes two main scenarios, weak chaos and robust chaos, according to the value of fractional order ν. When $\nu \in (0, 0.5)$, the MLE decreases towards 0, meaning that the fractional map (13) displays weak chaos. In contrast, when $\nu \in [0.5, 1]$, the MLE increases rapidly and takes positive values across this parameter ν range, then the fractional map (13) exhibits chaotic dynamic behavior, excepting a periodic window near $\nu = 0.81$ and $\nu = 0.98$. In this study, it is confirmed that the fractional map (13) has rich dynamics.

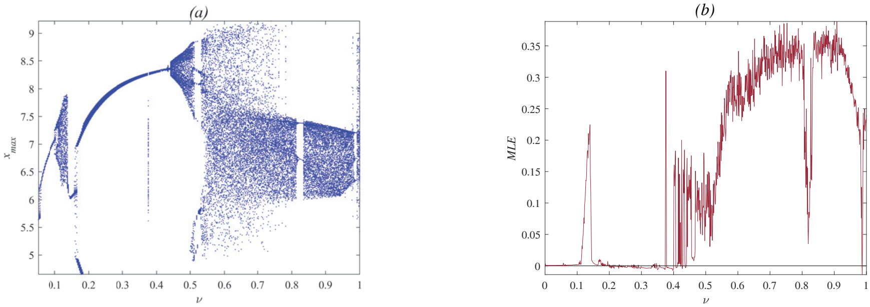

Figure 4: *Dynamics of the fractional-order map* (13) *as* ν *varies: (a) Bifurcation diagram with respect to* ν*; (b) Maximum Lyapunov exponent spectrum with respect to* ν.

To provide more clarification, the phase portrait of the fractional map (13) with different values of fractional order ν is plotted in Fig. 5.

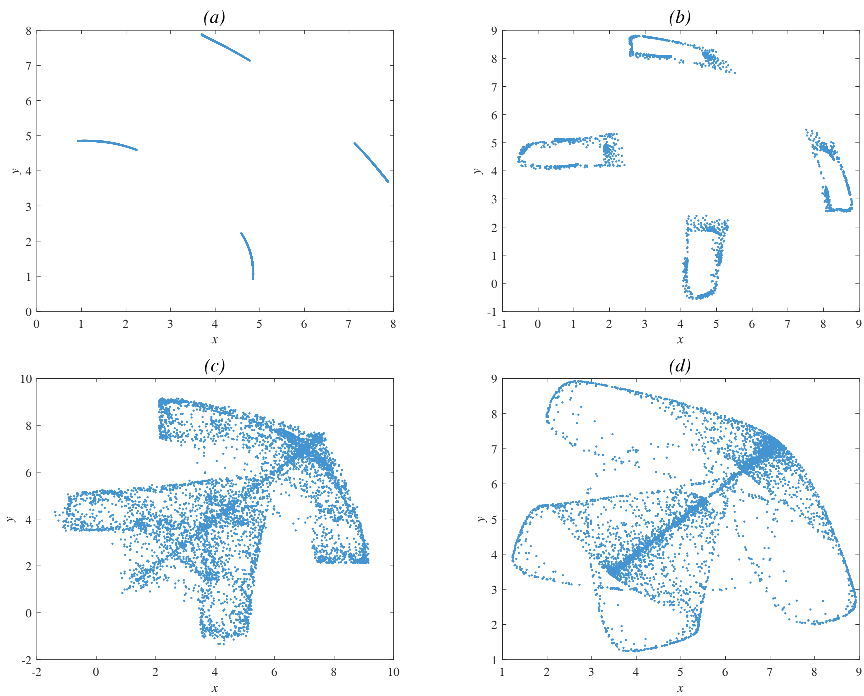

Figure 5: *Phase diagram of the fractional map* (13) *for different values of* ν*: (a) for* $\nu = 0.2$*; (b) for* $\nu = 0.5$*; (c) for* $\nu = 0.62$*; (d) for* $\nu = 0.99$.

As can be observed, the shape of the phase diagram of the fractional map (13) is changed according to the value of the fractional order ν. In particular, a strange attractor appears when the fractional map is chaotic. Thus, the fractional map (13) is sensitive to variation of ν, and the effect of the fractional order on the global dynamics of the fractional system (13) is investigated.

In order to examine how the fractional-order map (13) is influenced by the variation of the system parameters and fractional order ν, we use the chaos diagrams as shown in Fig. 6. In practical situations, a chaos diagram is useful for determining the suitable parameter values for real-world applications. Fix $\alpha = 2$, $\beta = 0.5$, and $\gamma = 0.5$, and let k vary from 0.6 to 0.9 with a step size of 0.001, and ν vary from 0 to 1 with a step size of 0.01. The colors in Fig. 6 represent the values of the maximum Lyapunov exponent when k and ν vary simultaneously. As can be observed, when the fractional order ν increases, the MLE is greater than zero in most of the areas, and the fractional map (13) exhibits chaotic behavior. In particular, when the fractional order closes 1, the fractional map (13) has complex dynamics. Thus, the impact of the system parameters and fractional order on the dynamical behavior of the fractional map (13) is investigated. As a result, the fractional discrete system (13) has rich dynamics when the system parameter k and the fractional order ν are varied.

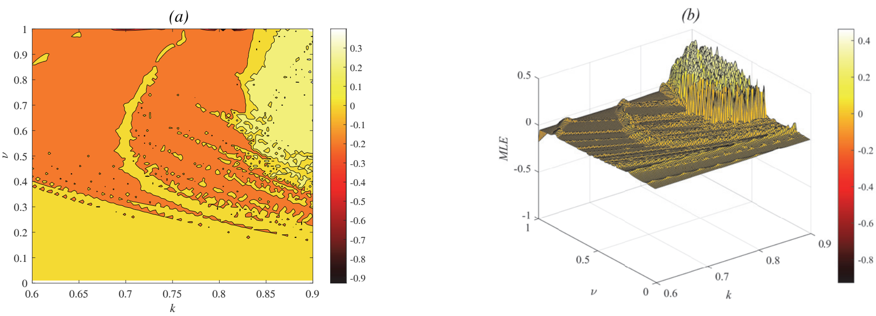

Figure 6: *Chaos diagram of the fractional-order map* (13) *based on the MLE: (a) in* 2*-D projection; (b) in* 3*-D projection.*

5. 0-1 test and complexity

5.1. 0-1 test for chaos

The 0-1 test technique is another method for establishing the existence of chaos in the fractional-order discrete system. The 0-1 test for chaos is a binary test that detects chaotic behavior in deterministic nonlinear systems, with the input being a time series of data and the output being 0 or 1, signifying either the dynamics are chaotic or not [20]. We provide a concise overview of the test algorithm's procedure. For a fractional-order system, if a set of discrete data $\phi(m)$ $(m = 1, 2, 3, \ldots)$ is a one-dimensional observable data set obtained from the iterative, we define the following two real-valued sequences:

$$\begin{aligned} p(m) &= \sum_{j=1}^{m} \phi(j)\cos(\omega(j)) \\ q(m) &= \sum_{j=1}^{m} \phi(j)\sin(\omega(j)), \end{aligned} \tag{15}$$

where

$$\omega(j) = j\varphi + \sum_{i=1}^{j} \phi(i), \tag{16}$$

and φ is a random constant selected from the interval $[\frac{\pi}{5}, \frac{4\pi}{5}]$. Plotting the trajectories in the (p,q)-plane provides a visual test, where the bounded trajectories of p and q imply regular dynamics, whereas the Brownian-like behavior (unbounded trajectories) imply chaotic dynamics. Next, we define the mean square displacement $M_\omega(m)$ as

$$M_\omega(m) = \lim_{N\to\infty} \frac{1}{N} \sum_{j=1}^{N} [p(j+m) - p(j)]^2 + [q(j+m) - q(j)]^2, \tag{17}$$

In practice, we compute $M_\omega(m)$ only for $m \leqslant m_{cut}$, where $m_{cut} = N/10$. Next, we define the asynchronous growth rate K_ω as

$$K_\omega = \lim_{m\to\infty} \frac{\log M_\omega(m)}{\log(m)}. \tag{18}$$

Finally, the growth rate K can be determined as

$$K = median(K_\omega). \tag{19}$$

If $K \approx 0$, it means that the dynamics are regular, whereas if $K \approx 1$, the dynamics are chaotic. Table 1 and Fig. 7 show the results of the 0-1 test for different values of fractional order ν. In particular, when $\nu = 0.2$, the trajectories in the (p,q)-plane show bounded behavior, then the system (13) is in a periodic state. In contrast, when $\nu = 0.5$, $\nu = 0.62$, $\nu = 0.89$, and $\nu = 0.99$, the trajectories in the (p,q)-plane show unbounded behavior, then the system (13) is mainly chaotic.

ν	0.2	0.5	0.62	0.89	0.99
K	0.0123	0.7007	0.9971	0.9967	0.9948

Table 1: *The asynchronous growth rate K of the fractional map (13) for different fractional order values.*

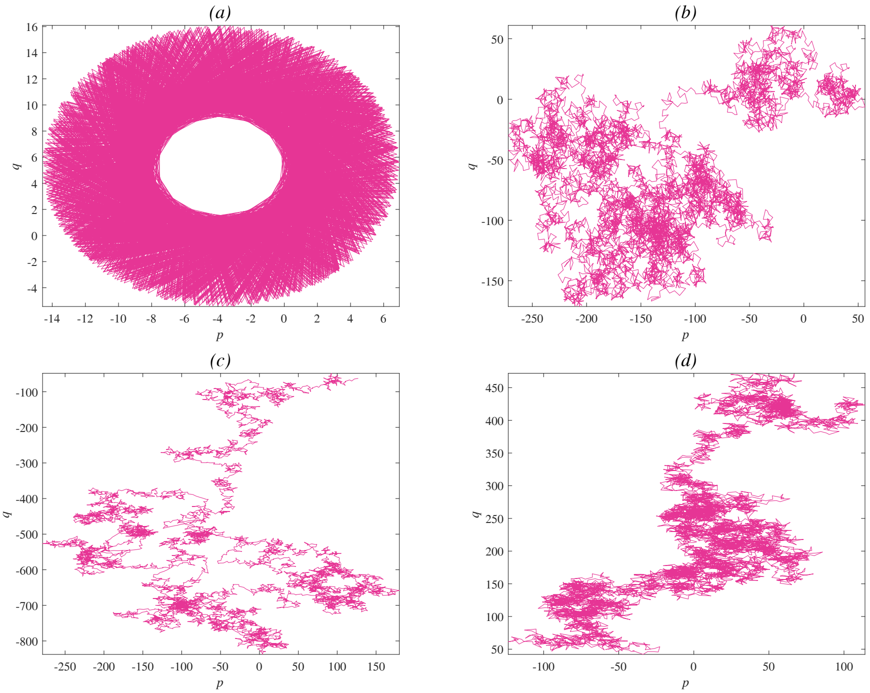

Figure 7: *Plotting of the* $p-q$ *trajectories of the fractional map* (13) *with different values of fractional order* ν*: (a) for* $\nu = 0.2$*; (b) for* $\nu = 0.5$*; (c) for* $\nu = 0.62$*; (d) for* $\nu = 0.99$.

5.2. C_0 algorithm

C_0 algorithm is an efficient algorithm used to measure the complexity level of a deterministic dynamical system [24]. Based on discrete data $x(m)$ $(m = 0, 1, 2, \ldots, N-1)$ selected from the ietrative, the corresponding discrete Fourier transformation is given by

$$X_N(k) = \sum_{m=0}^{N-1} x(m) \exp[-2\pi i \frac{km}{N}], \tag{20}$$

where $k = 0, 1, 2, \ldots, N-1$ and i is the imaginary unit. Next, we compute the mean square of X_N as

$$M_N = \frac{1}{N} \sum_{k=0}^{N-1} |X_N(k)|^2. \tag{21}$$

By introducing a control parameter r where

$$\tilde{X}_N(k) = \begin{cases} X(k) & \text{if} \quad |X_N(k)|^2 > rM_N, \\ 0 \quad \text{if} & |X_N(k)|^2 \leqslant rM_N, \end{cases} \tag{22}$$

the inverse discrete Fourier transformation is given by

$$\tilde{x}(m) = \frac{1}{N}\sum_{k=0}^{N-1}\tilde{X}_N(k)\exp[2\pi i\frac{km}{N}], \tag{23}$$

where $m = 0,1,2,\ldots,N-1$. Finally, the C_0 complexity is defined as

$$C_0(x,r,N) = \frac{\sum_{m=0}^{N-1}\|x(m)-\tilde{x}(m)\|^2}{\sum_{m=0}^{N-1}\|x(m)\|^2}. \tag{24}$$

Now, we apply the C_0 algorithm to the fractional map (13). Fig. 8 shows the C_0 complexity of the fractional system with respect to the fractional order ν.

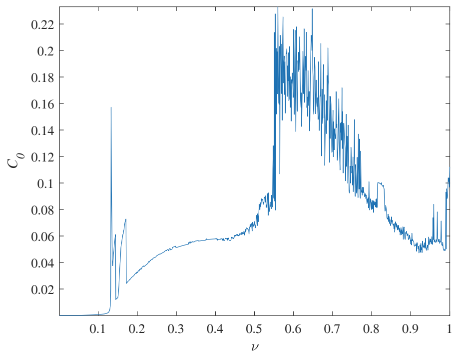

Figure 8: C_0 *complexity of the fractional map* (13) *with respect to* ν.

As one can see, the complexity of the fractional map (13) changes when the fractional order ν varies. In particular, the fractional map (13) has a high complexity level when $\nu \in [0.5, 0.8]$, which agrees well with the results of the bifurcation diagrams, maximum Lyapunov exponent spectrum, and 0-1 test. In practice, we must exercise caution when selecting the fractional order value, particularly if we require a high complexity level.

5.3. Spectral entropy

The spectral entropy (SE) is performed to evaluate the complexity of chaotic sequences in deterministic dynamical systems. We review briefly the steps of the this algorithm [14]. Consider a sequence of discrete data $x_1, x_2, \ldots, x_N$ selected from the iterative, and we delete the current part as

$$x(s) = x(s) - \frac{\sum_{m=1}^{N} x(m)}{N}, \tag{25}$$

where $s = 1, 2, \ldots, N$. Next, the correponding discrete Fourier transformation is given by

$$X_j = \sum_{s=1}^{N} x(s) \exp[\frac{-2\pi s j i}{N}], \tag{26}$$

where $j = 1, 2, \ldots, N$ and i is the unit imaginary. The probability of the power spectral density is defined as

$$p_j = \frac{|X_j|^2}{\sum_{j=1}^{N/2} |X_j|^2}. \tag{27}$$

Normalizing of the above quantity, then the spectral entropy is defined as

$$SE = \frac{\sum_{j=1}^{N/2} |p_j \log(p_j)|}{\log(N/2)}. \tag{28}$$

Now, we apply the SE algorithm to the fractional map (13) where the parameters are assigned as $\alpha = 2$, $\beta = 0.5$, $\gamma = 0.5$, $k = 0.87$, and let the fractional order ν vary from 0 to 1 with a step size of 0.01. Fig. 9 shows the spectral entropy of the discrete map (13) with respect to the fractional order ν.

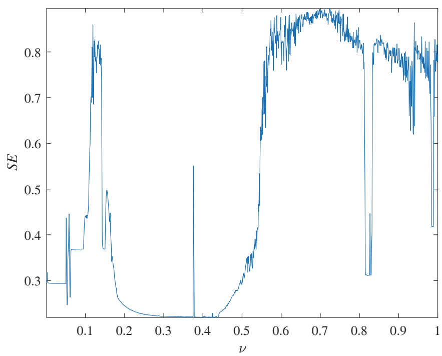

Figure 9: *Spectral entropy of the fractional map* (13) *with respect to fractional order* ν.

As can be observed, the complexity of the fractional map (13) is varied according to the fractional order ν. The SE complexity has a high level in the range $[0.5, 1]$, which agrees well with the result of the C_0 algorithm.

In order to examine the effect of the system parameters and fractional order on the global dynamics of the fractional map (13) more accurately, chaos diagrams based on the C_0 complexity and spectral entropy are depicted in Figs. 10(a) and 10(b), respectively. As we can see, the complexity of the fractional map (13) changes when the parameter k and the fractional order ν are varied. In particular, a high complexity is obtained when the parameter k approaches 0.85 and the fractional order ν ranges between $0.5 \leqslant \nu \leqslant 1$, which validates the results of the bifurcation diagrams, maximum Lyapunov exponent, and 0-1 test. Therefore, if more complex chaotic behavior is required in practical applications, the chaos diagrams can assist us in selecting the appropriate parameters and fractional order of the system.

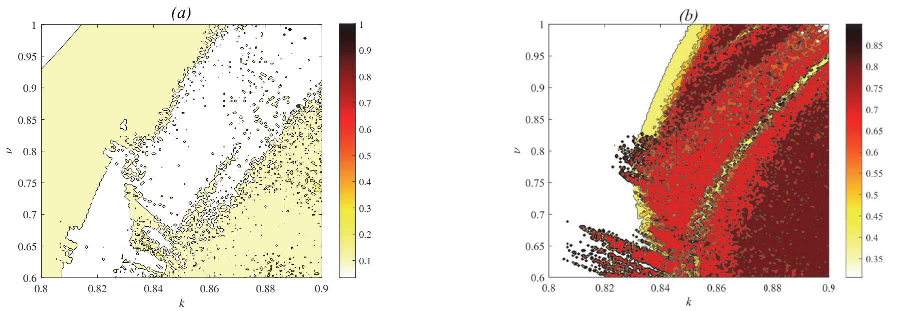

Figure 10: *Chaos diagram of the fractional map* (13) *on* (k,ν)*-plane: (a) based on* C_0 *complexity; (b) based on SE complexity.*

6. Controlling chaos

In this section, an active controller for stabilizing the state trajectories of the fractional map (13) is designed. Our goal is to force all states of the discrete system (13) to converge towards zero asymptotically.

THEOREM 3. *The fractional map* (13) *can be stabilized under the following two-dimensional control law*

$$\begin{cases} u_1(t) = -x(t) - y(t) - k(x(t))^2\left(\alpha - \gamma - \beta\frac{x(t)}{x(t)+y(t)} - \beta\log(x(t)+y(t))\right), \\ u_2(t) = -y(t) - k(y(t))^2\left(\alpha - \gamma - \beta\frac{y(t)}{x(t)+y(t)} - \beta\log(x(t)+y(t))\right). \end{cases} \tag{29}$$

where $t \in \mathbb{N}_{\theta+1}$.

Proof. The fractional map (13) with the control law (29) is expressed as

$$\begin{cases} {}^{C}\Delta_{\theta}^{\nu}x(t) = k(x(t-1+\nu))^2(\alpha-\gamma-\beta\dfrac{x(t-1+\nu)}{x(t-1+\nu)+y(t-1+\nu)} \\ \qquad -\beta\log(x(t-1+\nu)+y(t-1+\nu))) + u_1(t-1+\nu), \\ {}^{C}\Delta_{\theta}^{\nu}y(t) = k(y(t-1+\nu))^2(\alpha-\gamma-\beta\dfrac{y(t-1+\nu)}{x(t-1+\nu)+y(t-1+\nu)} \\ \qquad -\beta\log(x(t-1+\nu)+y(t-1+\nu))) + u_2(t-1+\nu). \end{cases} \tag{30}$$

where $t \in \mathbb{N}_{\theta+1-\nu}$. Next, we substitute (29) into (30), we obtain the simplified dynamics

$$\begin{cases} {}^{C}\Delta_{\theta}^{\nu}x(t) = -x(t-1+\nu) - y(t-1+\nu), \\ {}^{C}\Delta_{\theta}^{\nu}y(t) = -y(t-1+\nu), \end{cases} \tag{31}$$

where $t \in \mathbb{N}_{\theta+1-\nu}$. We can simplify (31) to the compact form as

$$ {}^{C}\Delta_{\theta}^{\nu}\,(x(t),y(t))^{T} = M \times (x(t-1+\nu),y(t-1+\nu))^{T}, \quad t \in \mathbb{N}_{\theta+1-\nu}, \tag{32}$$

where

$$M = \begin{pmatrix} -1 & -1 \\ 0 & -1 \end{pmatrix}. \tag{33}$$

The eigenvalues of the matrix M are $\lambda_1 = \lambda_2 = -1$, and we have

$$|\lambda_i| = 1 < \left(2\cos\frac{|\arg\lambda_i| - \pi}{2-\nu}\right) \quad \text{and} \quad |\arg\lambda_i| = \pi > \nu\frac{\pi}{2}, \quad i = 1,2. \tag{34}$$

Hence, we can conclude that the zero equilibrium of system (31) is asymptotically stable. Thus, the state trajectories of the fractional chaotic map (13) are stabilized. □

For numerical simulations, the parameters of the fractional map (13) are selected as $\alpha = 2$, $\beta = 0.5$, $\gamma = 0.5$, $k = 0.87$, and the fractional order as $\nu = 0.62$. The initial conditions are arbitrarily selected as $(x_0, y_0) = (0.21, 0.22)$. Thus, the fractional map (13) behaves chaotically. Fig. 11 shows the evolution of the state trajectories and phase portrait of the controlled fractional map (30). From Fig. 11, it is shown that the states $x(m)$ and $y(m)$ converge rapidly towards zero asymptotically. As a result, the fractional map (13) is stabilized under the control law (29).

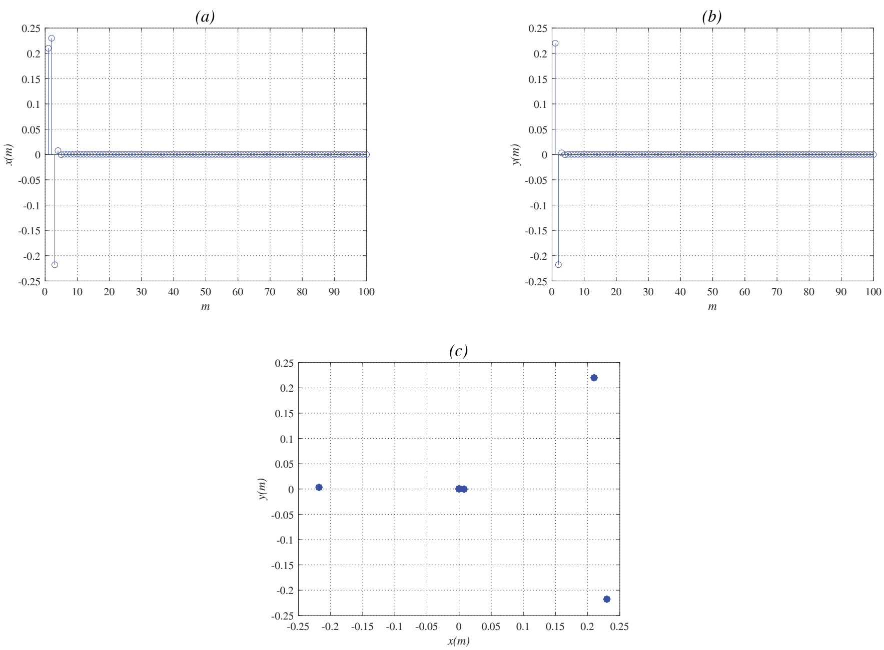

Figure 11: *State trajectories and phase portrait of the fractional map* (13) *after control: (a) Time series of* $x(m)$*; (b) Time series of* $y(m)$*; (c) Phase portrait in* (x,y)*-plane.*

7. Conclusions and future works

In this paper, a 2-D fractional map is presented. Using the Caputo-like difference operator, the fractional counterpart is constructed. We have shown that the proposed fractional map is sensitive to variation in both the bifurcation parameters and the fractional order. The effect of system parameters and fractional order is investigated using several classical tools, such as bifurcation diagrams, maximum Lyapunov exponent spectrum, chaos diagrams, and the 0-1 test algorithm. It is shown that the suggested map can exhibit chaotic behavior and complex dynamics. In addition, using the C_0 algorithm and spectral entropy technique, the complexity of the fractional map is quantified with accuracy. A high complexity level indicates that the fractional map has rich dynamics. Finally, we have designed a nonlinear control law for stabilizing the state trajectories of the chaotic map, where the controlled states converge towards the origin. MATLAB simulations were performed to illustrate and validate the theoretical results obtained in this paper.

In the near future, we will aim to apply the proposed fractional chaotic map in real-world applications, such as medical image encryption, signal processing, and secure communication.

REFERENCES

[1] T. ABDELJAWAD, *On Riemann and Caputo fractional differences*, Computers & Mathematics with Applications. **62**, 3 (2011), 1602–1611.

[2] S. S. ASKAR, *Complex dynamic properties of Cournot duopoly games with convex and log-concave demand function*, Operations Research Letters. **42**, 1 (2014), 85–90.

[3] F. ATICI AND P. ELOE, *Initial value problems in discrete fractional calculus*, Proceedings of the American Mathematical Society. **137**, 3 (2009), 981–989.

[4] S. BENSID AHMED, A. OUANNAS, M. AL HORANI AND G. GRASSI, *The Discrete Fractional Variable-Order Tinkerbell Map: Chaos, 0-1 Test, and Entropy*, Mathematics. **10**, 17 (2022), Art. No. 3173.

[5] J. ČERMÁK, I. GYŐRI AND L. NECHVÁTAL, *On explicit stability conditions for a linear fractional difference system*, Fractional Calculus and Applied Analysis. **18**, (2015), 651–672.

[6] M. F. DANCA, *Fractional order logistic map: Numerical approach*, Chaos, Solitons & Fractals. **157**, (2022), Art. No. 111851.

[7] W. FENG, Q. WANG, H. LIU, Y. REN, J. ZHANG, S. ZHANG, K. QIAN AND H. WEN, *Exploiting newly designed fractional-order 3D Lorenz chaotic system and 2D discrete polynomial hyper-chaotic map for high-performance multi-image encryption*, Fractal and Fractional. **7**, 12 (2023), Art. No. 887.

[8] J. GANCIO AND N. RUBIDO, *Lyapunov exponents and extensivity of strongly coupled chaotic maps in regular graphs*, Chaos, Solitons & Fractals. **178**, (2024), Art. No. 114392.

[9] A. GASRI, A. A. KHENNAOUI, A. OUANNAS, G. GRASSI, A. IATROPOULOS, L. MOYSIS AND C. VOLOS, *A New Fractional-Order Map with Infinite Number of Equilibria and Its Encryption Application*, Complexity. **2022**, 1 (2022), Art. No. 3592422.

[10] N. HANECHE AND T. HAMAIZIA, *A secure communication scheme based on generalized modified projective synchronization of a new 4-D fractional-order hyperchaotic system*, Physica Scripta. **99**, 9 (2024), Art. No. 095203.

[11] N. HANECHE AND T. HAMAIZIA, *A three-dimensional discrete fractional-order HIV-1 model related to cancer cells, dynamical analysis and chaos control*, Mathematical Modelling and Numerical Simulation with Applications. **4**, 3 (2024), 256–279.

[12] N. HANECHE AND T. HAMAIZIA, *The impact of the Caputo fractional difference operator on the dynamical behavior of a discrete-time SIR model for influenza A virus*, Physica Scripta. **99**, 11 (2024), Art. No. 115269.

[13] S. HE, H. WANG AND K. SUN, *Solutions and memory effect of fractional-order chaotic system: A review*, Chinese Physics B. **31**, 6 (2022), Art. No. 060501.
[14] S. HE, K. SUN AND H. WANG, *Complexity analysis and DSP implementation of the fractional-order Lorenz hyperchaotic system*, Entropy. **17**, 12 (2015), 8299–8311.
[15] T. HU, *Discrete Chaos in Fractional Henon Map*, Applied Mathematics. **5**, 15 (2014), 2243–2248.
[16] A. A. KHENNAOUI, A. OUANNAS, S. BENDOUKHA, G. GRASSI, R. P. LOZI AND V. T. PHAM, *On fractional-order discrete-time systems: Chaos, stabilization and synchronization*, Chaos, Solitons & Fractals. **119**, (2019), 150–162.
[17] M. H. KHOOBAN, M. GHEISARNEJAD, N. VAFAMAND AND J. BOUDJADAR, *Electric vehicle power propulsion system control based on time-varying fractional calculus: Implementation and experimental results*, IEEE Transactions on Intelligent Vehicles. **4**, 2 (2019), 255–264.
[18] T. LOOSSENS, F. TUERLINCKX AND S. VERDONCK, *A comparison of continuous and discrete time modeling of affective processes in terms of predictive accuracy*, Scientific reports. **11**, 1 (2021), Art. No. 6218.
[19] K. S. NISAR, M. FARMAN, M. ABDEL-ATY, AND C. RAVICHANDRAN, *A review of fractional order epidemic models for life sciences problems: Past, present and future*, Alexandria Engineering Journal. **95**, (2024), 283–305.
[20] J. RAN, *Identification of chaos in fractional chaotic map*, Advances in Difference Equations. **2020**, 1 (2020), Art. No. 228.
[21] M. ROOHI, M. P. AGHABABA, AND A. R. HAGHIGHI, *Switching adaptive controllers to control fractional-order complex systems with unknown structure and input nonlinearities*, Complexity. **21**, 2 (2015), 211–223.
[22] M. K. SHUKLA AND B. B. SHARMA, *Investigation of chaos in fractional order generalized hyperchaotic Henon map*, AEU-International Journal of Electronics and Communications. **78**, (2017), 265–273.
[23] V. E. TARASOV AND J. J. TRUJILLO, *Fractional power-law spatial dispersion in electrodynamics*, Annals of Physics. **334**, (2013), 1–23.
[24] S. WANG, S. HE, A. YOUSEFPOUR, H. JAHANSHAHI, R. REPNIK AND M. PERC, *Chaos and complexity in a fractional-order financial system with time delays*, Chaos, Solitons & Fractals. **131**, (2020), Art. No. 109521.
[25] H. WEITZNER AND G. M. ZASLAVSKY, *Some applications of fractional equations*, Communications in nonlinear science and numerical simulation. **8**, 3–4 (2003), 273–281.
[26] G. C. WU AND D. BALEANU, *Discrete fractional logistic map and its chaos*, Nonlinear Dynamics. **75**, (2014), 283–287.
[27] G. C. WU AND D. BALEANU, *Jacobian matrix algorithm for Lyapunov exponents of the discrete fractional maps*, Communications in Nonlinear Science and Numerical Simulation. **22**, 1–3 (2015), 95–100.
[28] G. C. WU, Z. G. DENG, D. BALEANU AND D. Q. ZENG, *New variable-order fractional chaotic systems for fast image encryption*, Chaos: An Interdisciplinary Journal of Nonlinear Science. **29**, 8 (2019), Art. No. 083103.
[29] G. C. WU, J. L. WEI AND T. C. XIA, *Multi-layer neural networks for data-driven learning of fractional difference equations' stability, periodicity and chaos*, Physica D: Nonlinear Phenomena. **457**, 1 (2024), Art. No. 133980.

(Received June 8, 2024)

Haneche Nabil
Applied Mathematics and Modeling Laboratory
Department of Mathematics, University of Mentouri Brothers
Constantine 25000, Algeria
e-mail: nabil.haneche@doc.umc.edu.dz

Hamaizia Tayeb
Mathematical Modeling and Simulation Laboratory
Department of Mathematics
University of Mentouri Brothers
Constantine 25000, Algeria
e-mail: el.tayyeb@umc.edu.dz